



On the microstructures of equilibrated and quenched spinel-containing nickel titanates

IAN M. ANDERSON†, C. BARRY CARTER‡ and HERMANN SCHMALZRIED§

Department of Chemical Engineering and Materials Science, Amundson Hall,
University of Minnesota, 421 Washington Avenue SE, Minneapolis,
MN 55455-0132, USA

[Received 28 May 1999 and accepted 14 July 1999]

ABSTRACT

Electron microscopy has been used to study the microstructures of equilibrated and quenched NiO–TiO₂ mixtures containing 5, 10, 15, 20 and 25 wt% TiO₂. All the specimens contained rocksalt- and spinel-structured phases on a nanometre scale. The microstructure suggests that a non-stoichiometric spinel decomposed during quenching. The 25 wt% TiO₂ specimen exhibited a lamellar microstructure composed of NiTiO₃ and spinel–NiO. These phases had the usual orientation relationships, i.e., $(111)_{\text{cubic}} \parallel (0001)_{\text{hex}}$ and $(110)_{\text{cubic}} \parallel (1100)_{\text{hex}}$. Faceted NiO solid-solution regions with coherent cube-on-cube interfaces with the spinel were found in the four specimens of lower TiO₂ contents. When large (15 and 20 wt% TiO₂), these regions were faceted cuboidal particles. With lower TiO₂ contents, these regions were no longer equiaxed and could be interconnected. The specimens were chemically homogeneous on a length scale of about 1 μm. Morphological evidence is presented to explain which part of the microstructure most probably already existed in this form during equilibration. In particular, the large-scale NiTiO₃ and the spinel lamella in the 25 wt% TiO₂ material form during long-term equilibration.

§ 1. INTRODUCTION

The close-packed oxides of the 3d transition metals, and elements of similar atomic radii, have contributed substantially to our understanding of simple ceramic systems. The ternary oxides of these elements tend to include phases having the structures of rocksalt (NaCl), corundum (Al₂O₃), rutile (R = TiO₂), spinel (S = MgAl₂O₄), ilmenite (ilm = FeTiO₃) and perovskite (CaTiO₃). Such phases have been employed as model systems for the study of basic science issues such as phase relations, point-defects, interface structure, etc., as well as physical properties such as electrical conductivity and magnetism. They have been extensively studied and many of their properties are well understood.

The spinel in the quasi-binary system NiO–TiO₂ does not obey the trends that characterize many known compounds with this structure. The most reliable compilation of the phase relations in the NiO–TiO₂ system is reproduced in figure 1 (Muan

† Present address: Metals & Ceramics Division, Oak Ridge National Laboratory, PO Box 2008, Oak Ridge, TN 37831-6376, USA.

‡ Author for correspondence. e-mail: carter@cems.umn.edu

§ Department of Physical Chemistry, University of Hannover, Hannover, Germany.

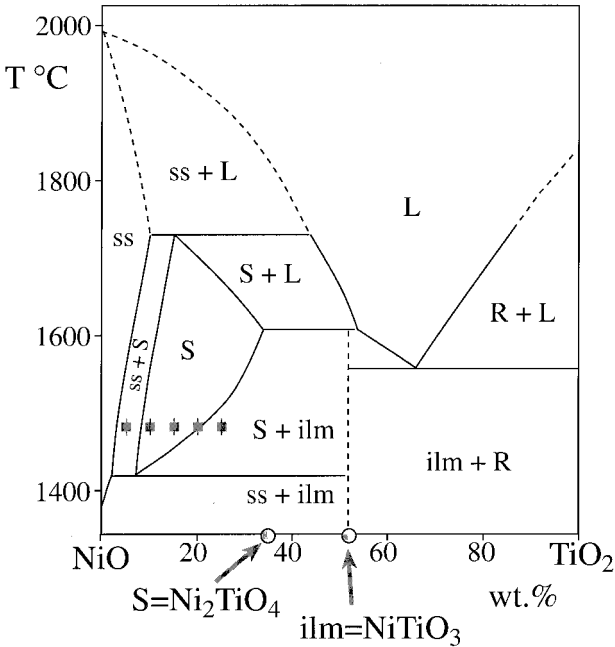


Figure 1. Phase relations in the system NiO-TiO₂, according to Muan (1992). A liquid phase (L) is shown in addition to the crystalline phases. In contrast to the phase relations reported by Laqua *et al.* (1977), a narrow two-phase region between distinct NiO(ss) and spinel(S) phases is reported. Also, the melting point of the ilmenite-structured (ilm) phase, NiTiO₃, is reportedly incongruent.

1992). These relations indicate the essential features of nickel titanate spinel: in air, it is stable only at elevated temperatures ($T > 1425^{\circ}\text{C}$); in the quasi-binary region ss + S it never reaches its hypothetical end-member, the stoichiometric spinel Ni₂TiO₄; and at its low-temperature stability limit it is closer in composition to NiO than to Ni₂TiO₄ (Laqua *et al.* 1977, Armbruster 1981, Muan 1992). However, some ambiguity has remained concerning the nature of this spinel compound because the high temperatures necessary to stabilize the phase make it very difficult to study it *in situ*. The present paper provides an analysis of the microstructures of spinel-containing specimens in the NiO-TiO₂ system which have been annealed at about 1480°C and then quenched.

§ 2. EXPERIMENTAL PROCEDURE

Five specimens in the system NiO-TiO₂ were equilibrated in air and rapidly quenched in cold water. These specimens were prepared as part of a larger study of phase relations (Muan 1992). Table 1 lists the designations of the specimens for this larger study, their compositions and equilibration temperatures. The locations of these specimens on the phase diagram are indicated in figure 1.

The loosely sintered powder specimens were prepared for electron microscopy examination after infiltrating the porous specimens with a low-viscosity epoxy. Specimens were examined by transmission electron microscopy (TEM) with a JEOL 1200EX operated at 120 kV. Scanning electron microscopy (SEM) was performed with a Hitachi S-900 equipped with a field-emission electron gun and operated at 3 kV.

Table 1. Specimens examined in this study.

Mixture (Muan 1992)	TiO ₂ content (wt%)	Equilibrium temperature (°C)
13	5	1483
4	10	1488
15	15	1483
5	20	1488
6	25	1483

§ 3. RESULTS

Representative microstructures of the four specimens with TiO₂ contents of 5–20 wt% were composed only of phases with the rocksalt and spinel structures, as shown in figure 2. The strong-beam (SB) dark-field (DF) images were formed with the spinel (220) reflection near the [001] zone axis common to the NiO(ss) and spinel-structured phases; in figure 1, NiO(ss) denotes NiO solid solution and S denotes the

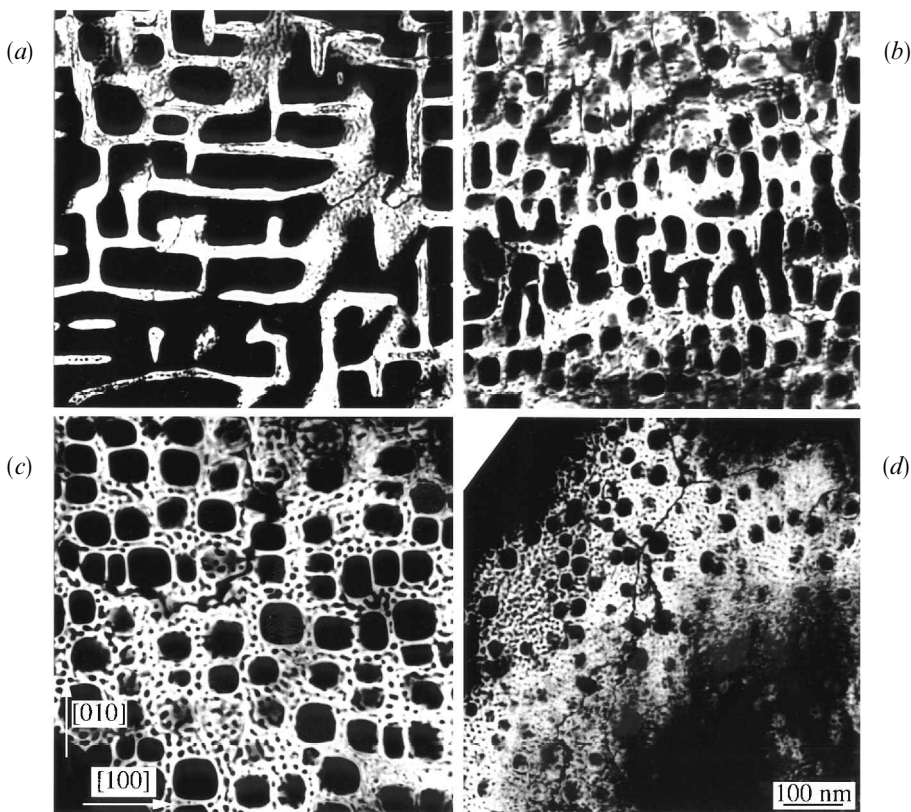


Figure 2. The microstructure of equilibrated and quenched specimens in the NiO–TiO₂ system with (a) 5, (b) 10, (c) 15, and (d) 20 wt% TiO₂. The specimens were equilibrated at 1483°C or 1488°C. These are DF TEM images formed with the spinel (220) reflection near the [001] pole, which is common to the two cubic phases. The spinel appears bright, and the NiO(ss) dark, in the images.

nickel titanate spinel. In the micrographs, the spinel appears bright and the NiO(ss) appears dark.

In the spinel-rich regions of the microstructure shown in figure 2 there are finely dispersed regions of NiO(ss) (a few nanometres across). There is no apparent texturing to this NiO(ss) and the scale of the modulations does not correlate with the TiO₂ mass fraction of the specimens. In its scale and morphology, this spinel–NiO(ss) dispersion arises from the decomposition which occurs during quenching of an initially homogeneous non-stoichiometric spinel. A selected-area diffraction (SAD) pattern representative of these specimens, shown in figure 3, indicates that the NiO(ss) and the spinel in these quenched specimens are near their stoichiometric compositions 'NiO' and 'Ni₂TiO₄'. If any significant non-stoichiometry had been retained during quenching, either diffuse reflections, indicative of randomly distributed point defects, or additional superlattice reflections, indicative of point-defect ordering, would be expected. Neither diffuse, nor superlattice, reflections are present in figure 3. (Diffuse reflections have been observed in X-ray diffraction (XRD) patterns of spinel-containing nickel titanates with ternary additions of MgO and CoO (De Graef *et al.* 1985).)

The microstructures in figure 2 are presumed to be nearly stoichiometric NiO and Ni₂TiO₄, which evolved during quenching from a non-stoichiometric spinel, and can be designated Ni_{2(1-x)}Ti_{1-x}O₄. This formula assumes that the cations are all of the oxidation states Ni²⁺ and Ti⁴⁺. The parameter *x* characterizes the degree of non-stoichiometry, or non-equimolarity, and is a substantial fraction of unity. At 1480°C, it ranges from 0.37 to 0.70, as can be deduced from the phase diagram.

The other principal feature of the microstructure is the NiO(ss) regions which are about 100 nm in size and lie between the spinel-rich regions. The size and volume fraction of these NiO(ss) regions decrease with increasing TiO₂ mass fraction. The interfaces between the spinel-rich and NiO(ss) regions tend to be faceted along {100} planes. In the 15 and 20 wt% TiO₂ specimens these NiO(ss) regions take the form of cuboidal particles distributed throughout the spinel-rich matrix. In the 5 and 10 wt%

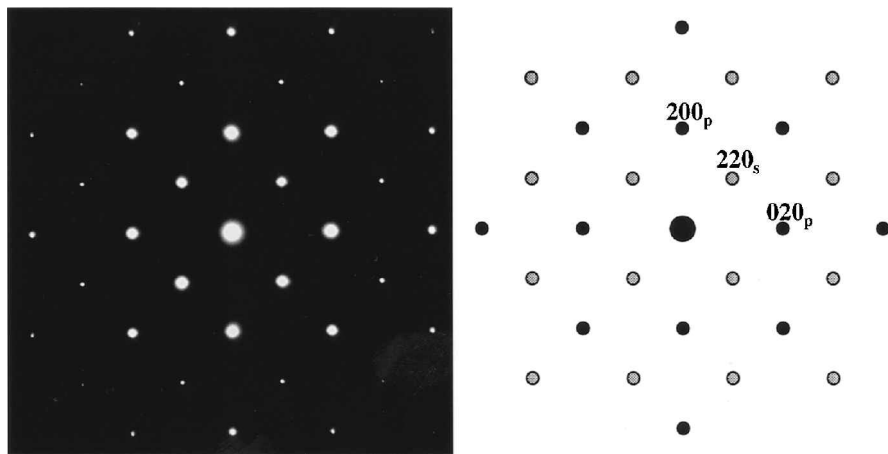


Figure 3. Selected-area diffraction pattern characteristic of the specimens shown in figure 2, together with a corresponding schematic. The pattern was recorded at the [001] pole of the cubic phases. The patterns of the two phases superimpose so that $(hkl)_p = (2h\ 2k\ 2l)_s$.

TiO₂ specimens the NiO(ss) regions are not equiaxed, and appear to form an interconnected network.

The microstructure of the specimen containing 25 wt% TiO₂ is shown in figure 4. The specimen is oriented near the [112] zone axis of the cubic phases, which is nearly coincident with the [1120] zone axis of the ilmenite phase; this phase is referred to hereafter as NiTiO₃. Figures 4(a) and (b) show SB DF images formed with the (1104) reflection of the NiTiO₃ and the (220) reflection of the spinel, respectively. The bright regions in the two images are (a) NiTiO₃ and (b) spinel. The NiO(ss) is the darkest of the three phases in both figures.

In this lamellar microstructure, alternate lamellae are composed of the hexagonal close-packed NiTiO₃ and the cubic close-packed spinel and/or NiO(ss). Some of the narrower lamellae are composed entirely of the NiO(ss). In the broader lamellae of the cubic close-packed oxides the regions adjacent to the NiTiO₃ lamellae tend to be NiO(ss), whereas the interior of the lamellae exhibit the nanometre-scale spinel and NiO(ss) seen in figure 2. Larger pockets of the NiO(ss) appear to emanate from the phase boundaries with the NiTiO₃, consistent with their nucleation during quenching, possibly from misfit dislocations at the phase boundary. In contrast to the larger NiO(ss) regions in figure 2, these pockets form relatively isotropic interfaces with the spinel.

A selected-area diffraction pattern from this region of the specimen is shown in figure 5. This SAD pattern indicates that the interfaces between the cubic- and hexagonal-close-packed oxides exhibit the usual low-energy epitaxial relationships, vis. $\{111\}_{\text{cubic}} \parallel \{0001\}_{\text{hex}}$, $\langle 110 \rangle_{\text{cubic}} \parallel \langle 1100 \rangle_{\text{hex}}$.

The phase boundaries between the lamellae are not strongly faceted. However, the presence of the NiO(ss) separating the spinel and NiTiO₃ lamellae indicates phase separation during quenching. Therefore, the relatively non-faceted interfaces

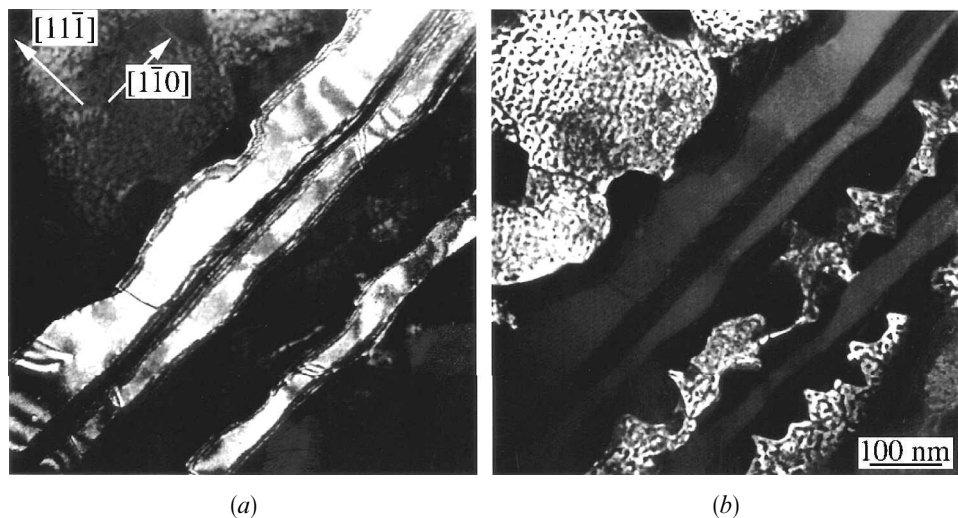


Figure 4. The microstructure of an equilibrated and quenched specimen with 25 wt% TiO₂. The specimen was equilibrated at 1483°C. It was oriented at the [112] pole of the cubic phases, which nearly coincides with the [1120] pole of the ilmenite-structured phase: (a) using (1104) reflection of the ilmenite-structured phase which thus appears bright; and (b) using (220) reflection of the spinel-structured phase which now appears bright. The NiO(ss) appears darkest in both images.

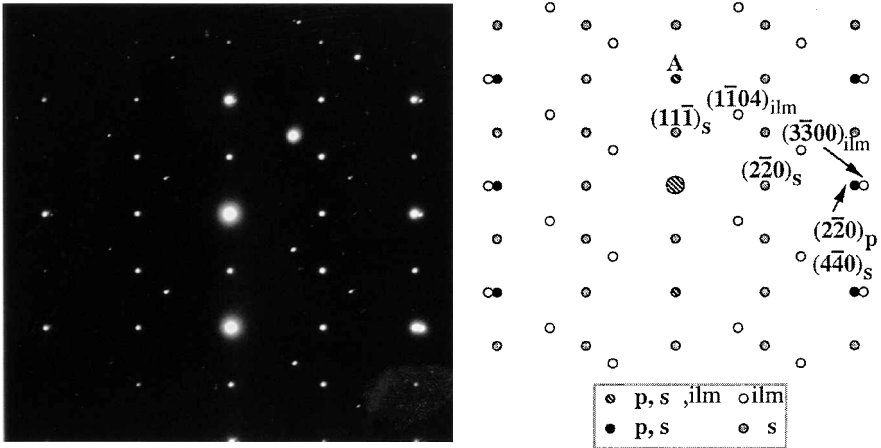


Figure 5. Selected-area diffraction pattern corresponding to the images in figure 4 together with the corresponding schematic. The pattern was recorded at the $[112]$ pole of the cubic phases, which nearly coincides with the $[1120]$ pole of the ilmenite-structured phase. The reflections $(0006)_{ilm}$ and $(\bar{1}11)_p / (222)_s$, labelled 'A', appear to superimpose. Reflections $(3300)_{ilm}$ and $(220)_p / (440)_s$ are collinear with the direct beam, but the former is displaced slightly further away than the latter.

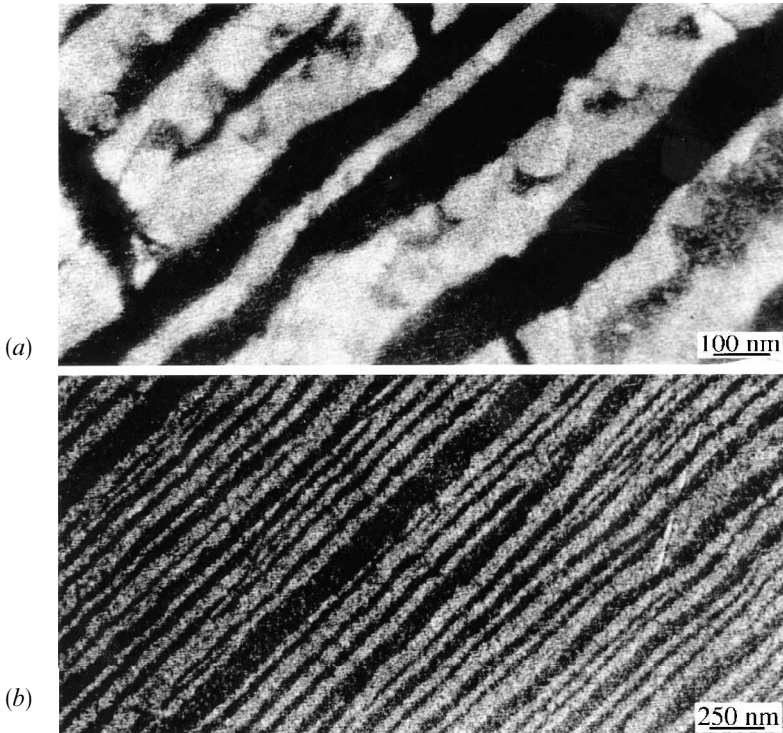


Figure 6. SEM images of the 25 wt% TiO_2 containing specimen showing families of lamellae. In these images, the $NiO(ss)$ appears brightest and the ilmenite-structure phases darkest. In (a) note the two distinct families of lamellae; and in (b) the lower magnification image shows lamellae lying on a single set of planes.

may have evolved during the quench. A larger area of the specimen, imaged with secondary electrons in a scanning electron microscope, is shown in figure 6. All of the microstructural features shown in the TEM image in figure 4 can also be seen in figure 6(a). In addition, figure 6(a) depicts a region of the two-phase specimen in which NiTiO₃ lamellae are oriented along two different {111} planes of the spinel. At places where the two families of lamellae intersect, the regions composed of the cubic oxides appear as parallelograms in the planar section imaged with the SEM. Figure 6(b) shows that colonies of lamellae extend over a large area of the specimen. The lamellar spacing varies, but has an average width of about 100 nm.

§ 4. DISCUSSION

A preliminary survey of the microstructural features of these specimens has been reported previously (Anderson *et al.* 1990). An earlier study of the microstructures of equilibrated and quenched spinel-containing nickel titanates was reported by DeGraef *et al.* (1985). These authors were able to show that specimens such as those in figure 2 were composed of both spinel and NiO(ss). Previous characterization of these specimens by XRD and electron probe microanalysis (EPMA) had incorrectly identified them as single-phase materials because of the perfect alignment of the two phases. The coherent phase boundaries between the two phases allowed their XRD patterns to be indexed as a single phase with space group $Fd\bar{3}m$, and the approximately 100 nm scale of the two-phase mixture made the specimens appear homogeneous on the scale of the resolution of EPMA (about 1 μm).

In contrast with the findings of the present study and a consideration of the correct phase diagram, De Graef *et al.* (1985) had concluded that there was a continuous transition with increasing TiO₂ content between the ~ 100 nm faceted and the ~ 5 nm isotropic NiO(ss) regions. The present study identifies these morphologies as distinct features of the microstructure, which are present to some extent in all specimens with sufficiently low TiO₂ content, so that the NiTiO₃ is absent. De Graef *et al.* also suggested, on the basis of high-resolution electron micrographs, that the interfaces between the NiO(ss) and spinel change from being abrupt in specimens with low TiO₂ content (as in figure 2(a)) to being continuous in specimens with higher TiO₂ content (as in figure 2(d)). However, the abrupt transition reported by these authors is characteristic of the faceted interfaces, imaged edge on, whereas the reported continuous transition between the two phases probably reflects the superposition of the nanometre-scale phase modulations through the thickness of the foil. The absence of either diffuse reflections or superlattice reflections in the SAD pattern (figure 3) indicates a low quenched-in point-defect concentration, which is inconsistent with such a continuous transition between the different phases.

The linear features seen in figure 2 are most probably antiphase boundaries (APBs). In the spinel, these planar defects do not, to a first approximation, affect the anion sublattice. They are, in effect, stacking faults on the cation sublattice. As such, they may influence the nucleation of NiO(ss) during quenching.

The reaction path during the cooling of the samples, as it follows from the phase diagram in figure 1, will be discussed next.

4.1. With 5 wt% TiO₂, $T(\text{eq}) = 1483^\circ\text{C}$

At the annealing temperature of 1483°C, the system is in the two-phase field NiO(ss) + spinel (= ss + S), but contains mainly ss. In the first stage of cooling to the eutectoid temperature, the NiO(ss) becomes poorer in TiO₂, i.e., spinel is precipi-

tated, adding to the spinel already present at the annealing temperature. After the system has cooled to below the eutectoid temperature, $T(\text{eut})$, the remaining spinel should decompose into NiO(ss) and NiTiO₃ according to the equilibrium phase diagram. However, formation of NiTiO₃ requires a significant structural rearrangement of the immobile O ions (pseudo-fcc to pseudo-hcp), and the available driving forces from undercooling are always small. Such driving forces are of the order of $(\Delta T/T)/\Delta H_{\text{trans}}$; typically ΔH is $\sim 10\text{--}20\text{ kJ mol}^{-1}$ in ionic materials when the transformation involves only cation rearrangement (Navrotsky and Schmalzried 1975). The observations show that instead of NiO(ss) and NiTiO₃, almost stoichiometric NiO and spinel, Ni₂TiO₄, are formed during decomposition, indicating that the transformation from fcc into hcp is a slow process, and that kinetics dictates the course of the reaction path. The nucleation of NiTiO₃ is avoided.

As can also be seen from the phase diagram, the non-stoichiometric stable spinel which exists at $T > T(\text{eut})$ contains a surplus of NiO which is exsolved during the cooling process. This exsolution below $T(\text{eut})$ accounts for small-sized NiO precipitates inside the spinel. If the spinel platelets, which originally were oriented mostly on {100} planes, are thin enough, the NiO is precipitated at the surface of the platelets, thus avoiding nucleation inside the spinel bulk. If the spinel plates are thicker, then often a depleted spinel zone can be seen near their surface, again due to the outward diffusion of Ni ions towards the NiO(ss)/S interface in order to avoid the nucleation of NiO in the bulk again.

The depleted zone is of the order of 10^{-6} cm; if it is assumed that the quench time is 2 s, the Ni diffusivity is $\sim 10^{-126}\text{ cm}^2\text{ s}^{-1}$. This is a most reasonable value for a diffusivity of a divalent cation in a spinel over a temperature range between 1200°C and 1300°C. Below this temperature, diffusion will be too slow.

4.2. With 10 wt% TiO₂, $T(\text{eq}) = 1488^\circ\text{C}$

From the phase diagram, it can be seen that this system is single phase before quenching. When the limit of the spinel field is crossed during cooling, NiTiO₃ should be exsolved and the remaining spinel should become richer in NiO until $T(\text{eut})$ is reached. However, for the same reason as outlined above, the formation of NiTiO₃ does not occur.

Below $T(\text{eut})$, the supersaturated spinel decomposes as before to give NiO and almost stoichiometric spinel; the amount of NiO to be precipitated is now much less than with the 5% TiO₂ sample, with the consequent changes in the microstructure, as can be seen from figure 2(b).

As long as the spinel is above $T(\text{eut})$ during cooling, the supersaturation in NiO is not high. Therefore, the nucleation of NiO in the spinel is correspondingly slow, leading to a small number of nuclei which eventually become large, and interconnected cuboid NiO precipitates. This occurs mainly below $T(\text{eut})$, where the supersaturation increases sharply, and further NiO is added to the already existing precipitates. Again, depleted zones form near the NiO/S interface with additional NiO precipitating in the spinel bulk.

Since, during quenching, the 15 wt% and 20 wt% TiO₂ samples both start from the single-phase spinel field, nothing is different in principle from the behaviour of the 10 wt% TiO₂ sample, except that the ratio NiO/S decreases. The microstructure reflects this decrease, as illustrated in figures 4(c,d).

Figure 2(a) showed spinel that was essentially exsolved from supersaturated NiO(ss) with NiO exsolved from this newly formed spinel below $T(\text{eut})$. By contrast,

for the samples shown in figure 4(b–d), NiO is always exsolved from supersaturated spinel. The precipitation of NiO(ss) above T(eut) and that below T(eut) should be distinguished, as already discussed.

4.3. With 25 wt% TiO₂, T(eq) = 1483° C

With this composition, the equilibrated sample is definitely located in the two-phase field spinel–NiTiO₃ before the quench, as can be seen from the phase diagram. Figures 4 and 6 indicate that the microstructure at T(eq) consists of lamellae of the spinel and the NiTiO₃ phases. During cooling to T(eut) the spinel becomes poorer in TiO₂ according to the phase diagram, and NiTiO₃ must precipitate out. This new precipitation can be seen in figure 4(a), where the precipitated NiTiO₃ is added to the surface of the initially existing NiTiO₃. The banding seen at the boundary between the M and N phases in figure 4(a) are diffraction-contrast thickness fringes which are present because the interface is inclined to the electron beam (Williams and Carter 1996).

After crossing T(eut), the non-stoichiometric spinel becomes unstable as discussed in § 4.1 and § 4.2, but again does not decompose into the equilibrium phases, i.e., NiO and NiTiO₃, but instead forms NiO and stoichiometric spinel, thus retaining its immobile oxygen sublattice.

Regions within the lamellae at which pockets of the NiO(ss) emanate from the interface with the NiTiO₃ may indicate a heterogeneous nucleation site for decomposition of the spinel, such as a misfit dislocation. The dimension of these pockets of NiO(ss), about 50 nm, can provide a realistic estimate of the typical diffusion length during quenching. Note also in figure 4 that the metastable spinel spans the lamellae in some places.

It can be seen that all the geometrical features of the microstructure of the specimens investigated can be explained consistently by the reaction path read from the phase diagram by Muan and given in figure 1. Two points, however, should be noted.

- (1) It was assumed that the (non-stoichiometric) spinel does not decompose below T(eut) into NiO(ss) and NiTiO₃ as the equilibrium diagram would suggest, but instead into NiO and Ni₂TiO₄. This decomposition is kinetically more favourable, is in line with Ostwald's rule, and is corroborated by experiment.
- (2) Demixing and decomposition are diffusive transport processes which need time. At some stage of the cooling process the systems lag behind their corresponding equilibrium values and eventually may be frozen in.

Kinetic data on cation redistribution in the sublattices and diffusion coefficients in similar systems give information on the freezing in. At about 1000°C, the relaxation time for the cation redistribution is of the order of one second (Becker and Rau 1992, Röttger and Schmalzried 1996, Baeckermann and Becker 1998). The measured chemical diffusion coefficient in the non-stoichiometric spinel Ni_{2–2x}Ti_{1+x}O₄ depends on x and T. At T = 1509°C, it is larger than 10^{–9} cm² s^{–1} (Laqua, *et al.* 1977). The self-diffusion coefficient of Ni²⁺ in the stoichiometric spinel is estimated to be of the order of 10^{–12} cm² s^{–1} at 1200–1300°C (Schmalzried 1971). These numbers ensure that, given the quench times of 2 s, below T(eut) there is enough time to homogenize the decomposed phases and to bring them close to the compositions which the equilibrium phase diagram of

Muan requires. The exception is the stoichiometric spinel, which forms as a metastable phase for kinetic reasons.

It is true that the driving forces for the decomposition process near T (eut) are small, as stated above. On the other hand, the fact that all the phases involved here are structurally similar, in particular those with the rocksalt and the spinel structure, indicates that the interfacial energies are also relatively small, so that the observed microstructures with their relatively large interfaces can develop.

The lattice parameters of the two cubic phases are well matched. Although the spinel phase has never been isolated from the NiO(ss), extrapolation of the lattice parameter of the two-phase mixture to the ideal endmember composition Ni₂TiO₄ suggests that the lattice mismatch with pure NiO is only about 0.1% (Armbruster 1981). Moreover, the oxygen sublattice of Ni₂TiO₄ is very nearly an ideal cubic close-packed array (as measured by the so-called oxygen parameter *u*).

§ 5. SUMMARY

The microstructures of equilibrated and subsequently quenched NiO–TiO₂ mixtures containing 5, 10, 15, 20 and 25 wt% TiO₂ have been examined by electron microscopy. The specimens up to 20 wt% TiO₂ were composed of NiO(ss) and almost stoichiometric spinel, often with small-scale NiO(ss) inclusions in the spinel phase. The NiTiO₃ phase expected from the phase diagram to occur in equilibrium with NiO(ss) has not been found in these samples, which indicates a kinetic impediment for the formation of NiTiO₃ during the short period of the quench.

In essence, all the morphological features found experimentally upon cooling are in agreement with the phase diagram as given by Muan (1992), and the corresponding reaction paths, with one exception: the non-stoichiometric spinel Ni_{2-2x}Ti_{1+x}O₄ is kinetically impeded from transforming into NiTiO₃. It decomposes instead into NiO and Ni₂TiO₄.

ACKNOWLEDGMENTS

This research was supported initially by the National Science Foundation under Grant DMR-8901218 and subsequently by the University of Minnesota 3M Harry Heltzer Chair. Some of the microscopy for this study was performed at the Cornell University Materials Science Center facility while the remainder was performed in the CIE Microscopy Facility; both establishments are supported in part by the National Science Foundation. The authors thank Professor S. Erlandsen for access to the Hitachi S-900 scanning electron microscope and Chris Frethem for technical assistance. Helpful discussions with the late Professor A. Muan, who suggested this study, are gratefully acknowledged. This research was performed while I.M.A. was a graduate student at Cornell University in the School of Applied and Engineering Physics.

REFERENCES

- ANDERSON, I. M., MUAN, A., and CARTER, C. B., 1990, *13th International Congress for Electron Microscopy* (San Francisco CA: San Francisco Press), p. 1058.
ARMBRUSTER, T., 1981, *J. Solid State Chem.*, **36**, 275.
BAECKERMANN, J., and BECKER, K. D., 1998, *Z. phys. Chem.*, **206**, 31.
BECKER, K. D., and RAU, F., 1992, *Ber. Bunsen Ges. Phys. Chem.*, **96**, 1017.
DE GRAEF, M. D., SEINEN, P. A., and IJDO, D. J. W., 1985, *J. Solid. State Chem.*, **58**, 357.

- LAQUA, W., SCHULZ, E. W., and REUTER, B., 1977, *Z. anorg. allg. Chem.*, **433**, 167.
- MUAN, A., 1992, *J. Amer. Ceram. Soc.*, **75**, 1357.
- NAVROTSKY, A., and SCHMALZRIED, H., 1975, *Festkörperthermodynamik* (Weinheim: Verlag Chemie).
- RÖTTGER, R., and SCHMALZRIED, H., 1996, private communication.
- SCHMALZRIED, H., 1971, *Werkstoffe und Korrosion*, **22**, 371.
- WILLIAMS, D. B., and CARTER, C. B., 1996, *Transmission Electron Microscopy: A Textbook for Materials Science* (New York: Plenum Press).